Bulletin of the Chemical Society of Japan, 2024, **97**, uoae096
https://doi.org/10.1093/bulcsj/uoae096
Advance access publication 17 September 2024

Articles

Highly efficient direct air capture using solid–liquid phase separation in aqueous diamine solution as sorbent

Furong Cao[1], Soichi Kikkawa[1], Hidetaka Yamada[2], Seiji Yamazoe[1,*]

[1]Department of Chemistry, Graduate School of Science, Tokyo Metropolitan University, Hachioji, Tokyo 192–0397, Japan

[2]Frontier Science and Social Co-creation Initiative, Kanazawa University, Kakuma-machi, Kanazawa, Ishikawa 920–1192, Japan

*Corresponding author: Department of Chemistry, Graduate School of Science, Tokyo Metropolitan University, Hachioji, Tokyo 192–0397, Japan.
Email: yamazoe@tmu.ac.jp

Seiji Yamazoe
Seiji Yamazoe received his PhD degree in 2008 from Kyoto University. That same year, he transferred to the Department of Materials Chemistry, Ryukoku University as an Assistant Professor and in 2012 was appointed as an Assistant Professor in the Department of Chemistry, the University of Tokyo. In 2017, he was promoted to Professor at Tokyo Metropolitan University. His current research interests include development of direct air capture system, synthesis of cluster catalysts for CO_2 conversion, and local structural studies on metal clusters using synchrotron-based spectroscopies.

Abstract

To reduce climate change, absorbing CO_2 directly from the air (DAC) with high-efficient CO_2 absorption, low-cost, and environmentally friendly system has been attracted much attention for several decades. In this work, a series of aqueous diamine solutions was examined for 400 ppm CO_2 absorption at ambient temperature. The absorbents exhibited CO_2 absorption with molar ratio of 1 mol_{CO2}/mol_{amine}, and aqueous isophorone diamine (IPDA) in particular showed >99% CO_2 removal even under a 500 mL min^{-1} flow of 400 ppm CO_2–N_2 with the contact rate of 13,761.5 h^{-1} between CO_2 and IPDA aqueous solution and the CO_2 absorption rate of 4.46 mmol/L min. A precipitate of carbamic acid of IPDA was formed by reaction with CO_2, and the CO_2 removal efficiency was enhanced by increasing the solution viscosity by the formation of this precipitate. The CO_2 was absorbed in aqueous IPDA solution as carbamic acid of IPDA and bicarbonate/carbonate species, and the absorbed CO_2 could desorb by heating under O_2-containing gas flow, which indicates our system is applicable to the CO_2 condensation for a plant growth. This work provides fundamental information to establishing a solid–liquid phase change system with a high-efficient and environmentally friendly DAC system using aqueous solvent.

Keywords: aqueous solvent, direct air capture, solid–liquid phase separation.

Graphical Abstract

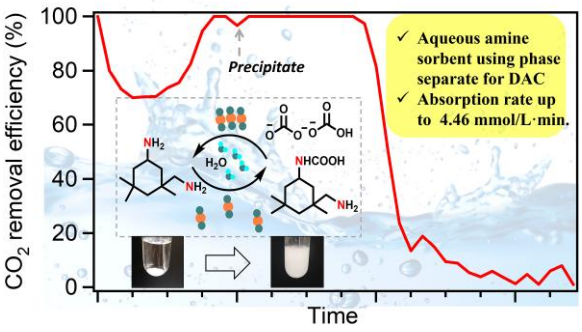

Aqueous diamine absorbent achieved very rapid low concertation CO_2 capture in solid-liquid separate.

1. Introduction

The fact that the rate of greenhouse gas emission now surpasses the natural removal rate has led to significant increases in the average temperature all over the world.[1] Excess atmospheric CO_2 is naturally removed through the soil, plants, seawater, and even rock; however, these CO_2 removal pathways are no longer sufficient due to exponential industrial development and the associated emission of CO_2 into the atmosphere. The atmospheric CO_2 concentration has increased by more than 45% from ca. 280 ppm in 1,880 to

[Received on 13 June 2024; revised on 7 September 2024; accepted on 10 September 2024; corrected and typeset on 26 September 2024]

>400 ppm at present, raising the average global temperature by 1.1 °C.[2] According to the Paris Agreement adopted in 2015, the increase in average global temperature should be kept below 2 °C compared with preindustrial levels, but to achieve this there is a need to remove CO_2 from the air via artificial means. Carbon capture and storage (CCS) is currently one of the most popular and acceptable ways of achieving net-zero CO_2 emissions.[3,4] CCS technology faces the major challenges of a high cost especially required for capture and the need to transport the captured CO_2 for storage. Further developments in CCS are thus required to increase the efficiency of CO_2 absorption and reduce energy consumption.

There are many kinds of technologies have been implemented to capture high-concentration CO_2 from gas flue, such as amine-based nanofluids.[5] However, those techniques have insufficient ability to capture low-concentration of CO_2. Thus, the further energy consumption is needed to capture CO_2 from the air since the CO_2 concentration should be increased by using membrane techniques to capture them by using the existing technologies.[6] CO_2 capture directly from ambient air (<500 ppm), so called direct air capture (DAC),[7,8] is a promising technology that can operate under very low concentrations of CO_2 gas.[9] Recent reviews have introduced the many advantages of DAC in detail, often focusing on the advantages of energy-saving and operational feasibility compared with conventional absorbents; notably, this approach can contribute to negative carbon emission technology.[10,11] In addition, DAC systems have inherent flexibility of placement and lower transportation costs compared with capturing CO_2 at stationary point sources. An ideal CO_2 absorbent for application in DAC system should use environmentally friendly reagents, achieve CO_2 absorption and desorption at a low cost, and have high absorption capacity, stability, and reusability. Moreover, the application of the captured CO_2 should be simultaneously discussed with DAC techniques. As the relationship between CO_2 concentration and plant growth have been studied,[12] greenhouse agriculture is one of the greatest markets for utilizing captured ambient CO_2.[13,14] The reported CO_2 concentration for the efficient plant growth, ca. 1000–1500 ppm, is slightly higher than ambient CO_2 concentration.[15,16] Thus, the cost-efficient and environmentally friendly DAC techniques are the promising for greenhouse agriculture (Fig. 1). In this DAC system, the CO_2-captured from ambient air is used for preparation high concentration CO_2. The challenges are the following points: lowering the desorption temperature of the captured CO_2 because there is no heat source in greenhouses, preventing the degradation of sorbents form oxidation as the supplied gas for the desorption contains O_2, and using environmentally friendly chemicals with low vapor pressure.

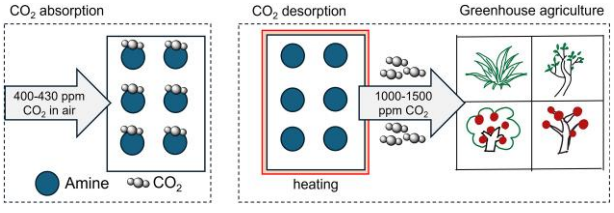

Fig. 1. Concept of DAC system to enhance the plant growing using concentrated CO_2.

To obtain a cost-efficient and environmentally friendly DAC system, many kinds of chemical absorbents have been developed. Amine-based absorbent is considered to be the most convenient and economical material for capturing CO_2 in industrial processes. Indeed, aqueous amine such as monoethanolamine (MEA) has been used for natural gas to capture high concentration CO_2 at high pressure since 1930,[17] while those are not for low concentration of CO_2. Thus, the development of the design of amine sorbents is demanded. Lipophilic amine and blended lipophilic amine were reported to show greater absorption and regeneration performance than MEA for high concentrations of CO_2 in postcombustion capture.[18] In addition, a pyrrolizidine-based system in polyethylene glycol efficiently captured air-concentration CO_2 at the ratio of one molar diamine to one molar CO_2 with the formation of a hexatomic ring between the amino group and CO_2.[19] Several aqueous alkanolamine solutions was effective to remove low-concentration CO_2 with a high yield of amine carbamate.[20] In addition, to remove low-concentration CO_2 in the air, it is reported that the CO_2 loading capacity of primary amine was higher than that of a secondary one both in aqueous and nonaqueous solutions.[21] In above-mentioned systems, aqueous solvents have huge advantages for industrial processes concerning their abundancy on the earth, environmental compatibility, and cost efficiency since H_2O vapor is a common component of air and almost all industrial gas streams that are rich in CO_2.[22] However, only a few articles have described aqueous solvent having sufficient absorption efficiency to capture low-concentration CO_2 in H_2O.

Some amine sorbents have been reported to form solid crystalline of carbamic acid or carbamate by CO_2 loading. Inagaki et al. have demonstrated that *m*-xylylenediamine (MXDA), *p*-xylylenediamine (PXDA), and *o*-xylylenediamine (OXDA) reacted with CO_2 in air and generated solid adduct at a molar ratio of amine to CO_2 of 1:1.[23,24] Elsewhere, Lewiński et al. demonstrated that the hydrogen-bond-mediated structures of CO_2-captured biguanide compounds differed between various organic and aqueous solvents.[25] The advantage of crystallization in the process is the separation of the solid phase from the sorbent solution. Custelcean group found that iminoguanidines, such as trichelating iminoguanidine, bis(iminoguanidine), glycine, and glyoxal-bis(iminoguanidine), having a positive charge that enables them to form salts with oxoanions as anion receptors, exhibited substantial CO_2-absorbing capacity by crystallization among guanidine amine, CO_2, and H_2O, and subsequent phase change.[26–29] The obtained crystals could release CO_2 by heating them, however, it required high temperature to desorb CO_2 due to the crystallization heat.

Recently, our group reported that a solid–liquid separation system with carbamic acid formation exhibited a high rate of CO_2 absorption and >99% removal of CO_2 at a low concentration, highlighting carbamic acid as a promising absorbent for DAC.[30] Besides, diamine compounds having a cyclohexyl skeleton demonstrated excellent CO_2 absorption capacity in DMSO at a molar ratio of CO_2 to amine of 1:1, while the adsorption capacity of MEA, a typical CO_2 removal reagent for high-concentration CO_2, was 0.5:1. Conventional liquid sorbents such as MEA did not show high CO_2 absorption capacity or absorption rate because the low concentration of CO_2 and formed carbamate species suppressed the forward reaction of CO_2 absorption [$R^1R^2NH(l) + CO_2(g) \Leftrightarrow R^1R^2NCOOH(l)$]. However, a solid–liquid phase change system overcame this

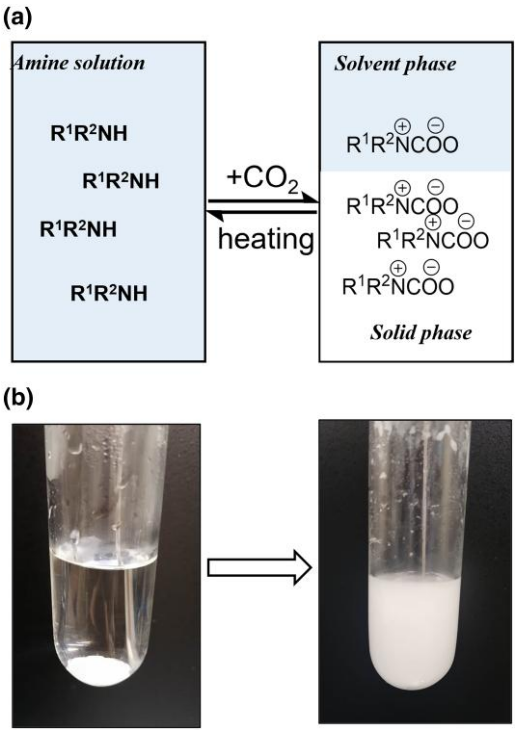

Fig. 2. a) Mechanistic scheme of the absorption and desorption cycle in a solid–liquid phase separation system. b) Photograph of solid product obtained in H_2O under 400 ppm CO_2–N_2.

limitation by equilibrium because the formed carbamic acid precipitated due to low solubility in DMSO [$R^1R^2NCOOH(l) \rightarrow R^1R^2NCOOH(s)$]; thus, the CO_2 absorption reaction was not suppressed (Fig. 2). We also found that the carbamic acid of IPDA could release all of the absorbed CO_2 in DMSO at 60 °C under a flow of N_2 and was reusable for absorption and desorption cycles. As the CO_2 was desorbed from liquid carbamic acid, the low desorption temperature was achieved by easy dissolution of solid carbamic acid into DMSO at low temperature. Thus, the use of solvent is a potential way to reduce the temperature for CO_2 desorption.

To establish a more environmentally friendly adsorbent system, this work focuses on the use of aqueous amine solutions as highly efficient absorbents under air-concentration CO_2. Among various diamines, the amine with a cyclohexane skeleton bearing two primary amino groups exhibited high stability and absorption capacity. Aqueous IPDA efficiently removed low-concentration CO_2 with >99% efficiency under a high flow of 400 ppm CO_2–N_2 and formed carbamic acid of IPDA as a precipitate and bicarbonate/carbonate ions in solution. The captured CO_2 could be released and concentrated up to 1.6% at 90 °C even under a flow of 20% O_2–N_2. This work revealed the relationship among CO_2 absorption efficiency, amine structure, and viscosity of solution, and provides a potential for establishing a solid–liquid phase change system for environmentally friendly DAC using aqueous solvent and applicability of our system to CO_2 condensation for plant growth.

2. Experimental

2.1 Chemicals

All chemicals were purchased and used without further purification. The following were purchased from Tokyo Chemical Industry Co., Ltd.: 3-(aminomethyl)-3,5,5-trimethylcyclohexylamine (isophorone diamine, IPDA; cis/trans mixture, >99.0%); 1,2-cyclohexanediamine (cis/trans mixture, >98%); 1,3-cyclohexanediamine (cis/trans mixture, >95%); 1,4-cyclohexanediamine (cis/trans mixture, >97%); 4,4′-methylenebis-(2-methylcyclohexylamine) (cis/trans mixture, >99%); 4,4′-methylenebis-(cyclohexylamine) (mixture of isomers, >97%); 1,3-bis(aminomethyl)cyclohexane (cis/trans mixture, >98%); 1,4-bis(aminomethyl)cyclohexane (>98%); *m*-xylylenediamine (>99%); *p*-xylylenediamine (>99%); sodium hydroxide (>98%); trans-*N*,*N*′-dimethylcyclohexane-1,2-diamine (>98%); *N*,*N*′-dicyclohexyl-1,2-ethanediamine hydrate (>98%); 1,6-diaminohexane (>99%); 1,2-diaminopropane (>98%); tris(2-aminoethyl)amine (>98%); piperazine anhydrous (>98%); 1-methylpiperazine (>98%); trihexylamine (>98%); dihexylamine (>98%); ethylenediamine (>89%); 1,3-diaminopropane (>98%); and diethylenetriamine (98%). Acetone and deuterium oxide (99.8%) were purchased from Kanto Chemical Co., Inc.

2.2 CO_2 absorption and desorption

A typical CO_2 absorption and desorption procedure is presented below and a schematic of the CO_2 absorption-desorption experimental apparatus is shown in Supplementary Fig. S1. Amine was put into the reactor and then solvent was added. A gas mixture of 400 ppm CO_2 diluted with N_2 was bubbled into the solution at ambient temperature with a set flow rate. Here, 1% CO_2–N_2 was used as absorption gas in the investigation of the absorption–desorption cycle capacity. A magnetic stirrer was used to speed up the contact between liquid and gas. The CO_2 concentration was monitored using a CO_2 probe (GMP 252, Vaisala GmbH) downstream of the sorbent. The CO_2 analyzer was calibrated using pure N_2 and standard CO_2 gas before the experiment.

CO_2 removal efficiency, r_{CO2} (%), was calculated from the CO_2 concentration of flow gas at the downstream of the reactor using the following equation (Equation 1):

$$r_{CO2}(\%) = 100\% \times \frac{1 - C_{t,\,CO2}}{C_{CO2}} \quad (1)$$

where $C_{t,CO2}$ is the downstream concentration of CO_2 at a certain time t and C_{CO2} is the concentration of CO_2–N_2 gas used. The amount of absorbed CO_2 was calculated by subtracting the amount of CO_2 accumulated without sorbent as a blank (S_{blank}) from the monitored amount of CO_2 accumulated downstream of the sorbent as an apparent value (S_{app}) as follows (Equation 2):

$$S_{abs}(\text{mmol}) = S_{app} - S_{blank} \quad (2)$$

The value of S_{app} can be calculated by the following equation (Equation 3):

$$S_{app} = \int_0^t C_{co2}(t)\mathrm{d}t \times F_{gas} \quad (3)$$

where F_{gas} refers to the flow rate of CO_2–N_2 gas. The contact rate between IPDA solution and gas is represented as space velocity (SV) and can be calculated using the following equation (Equation 4):

$$SV = \frac{F_{gas}}{V} \quad (4)$$

where V refers to the summed volumes of amine and solvent solution.

For the desorption of captured CO_2, 400 ppm CO_2–N_2 was sufficiently supplied into 1 mmol IPDA in 2.0 mL of H_2O, after which the mixture was heated under N_2 or 20% O_2–N_2 at a flow rate of 50 mL/min. The temperature was set at 50–90 °C and the desorption time was kept at 90 min.

The absorption and desorption cycles were also investigated over 1 mmol IPDA in 10 mL of H_2O. Absorption was carried out under 75 mL/min of 400 ppm CO_2–N_2 at room temperature. For the desorption experiment, the gas was changed to 50 mL/min N_2 at 90 °C for 90 min. The absorption and desorption were repeated for five cycles.

2.3 Characterization of CO_2 absorbed aqueous IPDA solution and carbamic acid (CA1) solid

The solid precipitate resulting from the reaction between IPDA and CO_2 was analyzed by ^{13}C NMR, FT-IR, and thermogravimetry. The solid precipitate that appeared in aqueous solution of amine after CO_2 absorption was washed with acetone, collected by centrifugation (2,000 rpm, 5 min, and three times), and dried under a vacuum at room temperature overnight. The ^{13}C NMR spectra of aqueous solution of IPDA after CO_2 absorption and desorption were measured by a Bruker AV500 spectrometer (125.77 MHz, ^{13}C NMR) with the addition of D_2O. The FT-IR spectra were measured using an FT-IR spectrometer (JASCO, FT/IR-4700) equipped with an attenuated total reflectance-infrared (ATR-IR) spectroscope (JASCO, ATR-PRO ONE). The desorption of CO_2 from the solid precipitate was measured using a thermogravimetric analyzer (Bruker, TG-DTA2000SA). The temperature was increased from 25 °C to 300 °C at a rate of 10 °C/min under N_2 flow, after which the temperature was held for 60 min. The viscosity of IPDA and **CA1** in solvent was analyzed using a tuning fork viscosity meter (A&D Company, SV-10A). A total of 30 mL of aqueous solution of amines was used for the measurement. The change in viscosity with time during CO_2 absorption was measured under a flow of 100% CO_2–N_2.

The solubility of the solid precipitate of carbamic acid resulting from the reaction between amine and CO_2 was estimated by measuring the mass of precipitate obtained in different amounts of solvent using a gravimetric method. After 0.214 g of **CA1** (ca. 1 mmol of carbamic acid) was dispersed in a certain amount of H_2O, the mixture with solid was strained through filter paper. The crude product was washed with acetone (5 mL and three times), after which the solid was dried in the air and then weighed. The molar amount was calculated by assuming that the reaction of IPDA with CO_2 proceeded at a 1:1 ratio.

2.4 Theoretical calculations for CO_2 absorption by IPDA

Transition state (TS) optimizations and intrinsic reaction coordinate (IRC) calculations were performed for the aqueous phase by density functional theory (DFT) at the B3LYP/6-311++G(d,p) level with the SMD solvation model using the integral equation formalism polarizable continuum model protocol for bulk electrostatics.[31] This level of theory has been shown to be applicable to similar amine–H_2O–CO_2 systems by previous studies.[32,33] The reactants and products obtained from the IRC calculations were optimized at the same level. Vibrational analyses were also applied to all stationary points to calculate their Gibbs free energies under the conditions of 1.0 atm and 298.15 K, and to confirm the absence or presence of only one imaginary frequency. As the initial structure for the reaction analysis, the most stable conformer of IPDA was selected based on the conformation search calculation using the MMFF94 molecular mechanics force field. All DFT calculations were performed using the Gaussian16 program.[34]

3. Results and discussion

First, a series of amines was screened to identify a suitable aqueous amine sorbent for a low concentration of CO_2. The capacity for absorbing 400 ppm CO_2 (S_{abs}) and the durability (time during which CO_2 removal efficiency exceeded 90%, T_{90}) are summarized in Table 1, Supplementary Table S1, and Supplementary Fig. S2. All diamines tested in this work exhibited a capacity to remove CO_2 of ~1 $mmol_{CO2}/mmol_{amine}$, regardless of the position of the amino groups. Meanwhile, IPDA maintained >90% removal efficiency for the longest time (Entry 1). Among the diamines tested in this work, 1,2-cyclohexanediamine, 1,3-bis(aminomethyl)cyclohexane, and 1,4-bis(aminomethyl)cyclohexane showed relatively long T_{90}. Some diamine absorbents, such as IPDA, MXDA, PXDA, 4,4′-methylenebis-(2-methyl-cyclohexylamine), and 4,4′-methylenebis-(cyclohexylamine), yielded a white solid in H_2O as a result of CO_2 absorption. There appeared to be no relationship between T_{90} and the formation of precipitate. Thus, the solubility of **CA1** formed by capturing CO_2 was not the only reason for IPDA's high efficiency of removal of CO_2 at a low concentration.

Next, we optimized the absorption reaction conditions of aqueous solution of IPDA (IPDA aq.) with low-concentration CO_2. Figure 3 shows the CO_2 removal efficiency over IPDA aq. with different flow rates of 400 ppm CO_2–N_2. IPDA aq. maintained >99% efficiency for 12 h under 400 ppm CO_2–N_2 at a flow rate of 75 mL/min and the total absorbed CO_2 reached 1.03 mmol (S_{abs} = 1.03 $mmol_{CO2}/mmol_{amine}$). The white precipitate appeared after ca. 4 h, which had signals at 164.9 (-NH**C**OOH) and 161.2 ppm ($H\mathbf{C}O_3^-/\mathbf{C}O_3^{2-}$) in ^{13}C NMR and absorption bands representing a carboxyl group (−COOH, 1600–1660 cm^{-1}) and an acetamide group (−NH–CO−, 1500–1600 cm^{-1}) in the FT-IR spectrum. This revealed the formation of carbamic acid of IPDA [**CA1**, 3-(aminomethyl)-3,5,5-trimethylcyclohexyl)carbamic acid) containing bicarbonate/carbonate species in the solution (Supplementary Figs. S3 and S4). As reported in our previous paper, dimethylsulfoxide (DMSO) solution of IPDA to react with CO_2 achieved 95% removal efficiency at begging stage and then achieved to 99% under 400 ppm CO_2–N_2 supplied at a flow rate of 75 mL/min.[23] Thus, we consider that IPDA has the potential for highly efficient CO_2 removal in aqueous solution. During the first 2 h supply of 400 ppm CO_2–N_2 at a flow rate of 175 mL/min, IPDA aq. showed 80% CO_2 removal efficiency, which correspond to 0.3 $mmol_{CO2}$, and then the efficiency improved to >99% accompanied by formation of carbamic acid. A flow rate of 400 ppm CO_2 hardly affected the CO_2 absorption capacity of IPDA (S_{abs}). For 400 ppm CO_2–N_2 supplied at a flow rate of 500 mL/min, the removal efficiency increased 1.4 times after precipitate formation. Remarkably, IPDA aq. exhibited >99% CO_2 removal under the supply of 400 ppm CO_2–N_2 at 500 mL/min, and the high removal efficiency also maintained under compressed

Table 1. CO_2 adsorption properties of various diamines in aqueous solution for 400 ppm CO_2–N_2[a].

Entry	Amine	Structure	Precipitate	T_{90} (min)	S_{abs} $mmol_{CO2}/mmol_{amine}$
1	IPDA	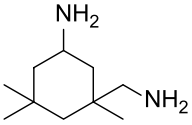	Formed	726	1.03
2	1,2-Cyclohexanediamine	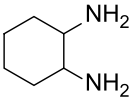	n.d.	388	1.00
3	1,3-Cyclohexanediamine	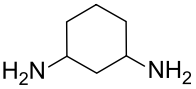	n.d	2	1.07
4	1,4-Cyclohexanediamine	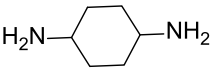	n.d	2	1.01
5	1,3-Bis(aminomethyl)cyclohexane	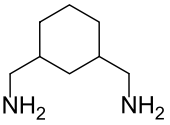	n.d	397	1.18
6	1,4-Bis(aminomethyl)cyclohexane	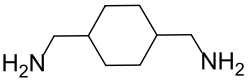	n.d	561	1.23
7	4,4′-Methylenebis-(2-methylcyclohexylamine)	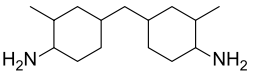	Formed	65	1.09
8	4,4′-Methylenebis-(cyclohexylamine)	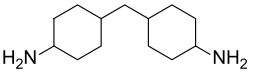	Formed	27	1.26
9	MXDA	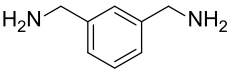	Formed	2	1.07
10	PXDA	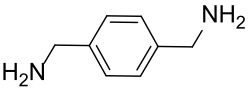	Formed	441	1.28

[a]CO_2 absorption ability was evaluated by flowing 400 ppm CO_2–N_2 gas through an aqueous solution of various diamines. Conditions: F_{gas}: 75 mL/min; amines: 1 mmol; H_2O: 2 mL; temperature: ambient.

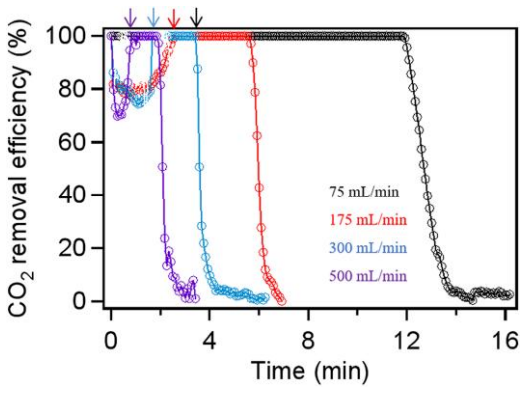

Fig. 3. CO_2 removal efficiency over an aqueous solution of 0.5 mol/mL H_2O IPDA under different gas flow rates of 400 ppm CO_2. The solid precipitate appeared at the point shown by color-coded arrow. IPDA: 1 mmol; H_2O: 2 mL; F_{gas}: 400 ppm CO_2–N_2, 75–500 mL/min; temperature: ambient. Black: 75 mL/min (S_{abs} = 1.03); red: 175 mL/min (S_{abs} = 1.05); blue: 300 mL/min (S_{abs} = 1.08); purple: 500 mL/min (S_{abs} = 1.06).

air (Supplementary Fig. S5). The CO_2 absorption rate (R_{SV}) reached 4.46 mmol/L min at a high contact rate between IPDA solution and gas (SV = 13,761.5 h^{-1}), which is the highest efficiency reported in the literature, such as for pyrrolizidine,[19] *m*-xylyenediamine,[24] MEA,[20] 2-(aminoethoxy)ethanol (DGA),[20] and 2-(amino-2-methyl-1-propanol) (AMP)[20] (Supplementary Table S2). We also tested the CO_2 absorption with just a contacting 400 ppm CO_2–N_2 with the surface of sorbent solution (Supplementary Fig. S6), as the pressure drop due to gas bubbling into the sorbent is a serious energy loss for developing a practical DAC system. Remarkably, CO_2 removal efficiency reached ca. 80% even at 150 mL/min flow of 400 ppm CO_2–N_2 at the gas–liquid contact area of 38.5 cm^2 without any gas bubbling, leading to CO_2 absorption rate (R_{Area}) from 400 ppm CO_2–N_2 of 32.6 mmol/h/m^2, which is comparable to the reported systems (ca. 14–144 mmol/h/m^2).[35]

The effect of IPDA concentration was tested over various H_2O contents of IPDA aq. Figure 4a shows the CO_2 removal efficiency over IPDA aq. that 1 mmol of pure IPDA was

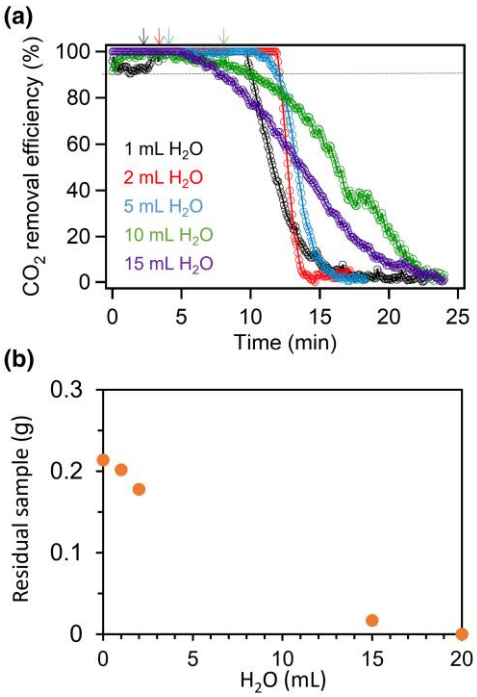

Fig. 4. a) CO_2 removal efficiency over various concentrations of aqueous solution of IPDA. IPDA: 1 mmol; H_2O: 1–15 mL; F_{gas}: 400 ppm CO_2–N_2, 75 mL/min; temperature: ambient. Black: 1 mL (T_{90} = 612 min, S_{abs} = 0.97); red: 2 mL (T_{90} = 726 min, S_{abs} = 1.03); blue: 5 mL (T_{90} = 713 min, S_{abs} = 1.07), green: 10 mL (T_{90} =587 min, S_{abs} = 1.28); purple: 15 mL (T_{90} = 460 min, S_{abs} = 1.11). b) Residual sample amount after dissolution of **CA1** (0.214 g, 1 mmol as $(CH_3)_3C_6H_4(NH_2)CH_2NHCOOH$(s)) into H_2O against H_2O volume. The solubility of **CA1** in H_2O was calculated as 11.20 g/L. **CA1** was obtained from IPDA with loading of CO_2, followed by washing with acetone.

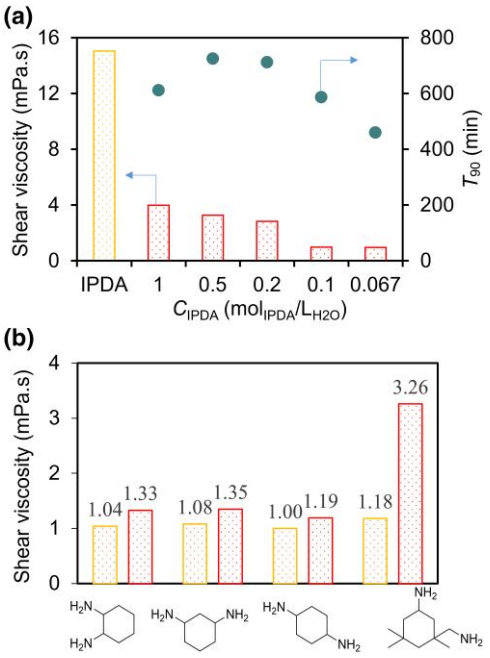

Fig. 5. a) Shear viscosity and T_{90} of IPDA aqueous solutions with various concentrations after sufficient CO_2 absorption. C_{IPDA} represents the concentration of IPDA in aqueous solution. Shear viscosity of IPDA before CO_2 loading was 15.05 mPa s. b) Shear viscosity of aqueous amines solutions of 0.5 mol_{amines}/mL_{H2O} (1,2-cyclohexanediamine, 1,3-cyclohexanediamine, 1,4-cyclohexanediamine, and IPDA) before (yellow) and after (red) absorption of sufficient CO_2.

diluted with 1–15 mL of H_2O. When the H_2O content was reduced to 1 mL, an induction period appeared for an initial 3 h, while S_{abs} was hardly affected. The keeping time for high reaction rate (T_{90}) increased with increasing the concentration of IPDA (SV = 3813.6 h^{-1} for 1 mL of H_2O and SV = 868.7 h^{-1} for 5 mL of H_2O). When IPDA aq. was used with 5 mL of H_2O, > 99% efficiency was maintained for 10 h, after which the efficiency gradually decreased. A further increase in H_2O content resulted in IPDA aq. with low viscosity and >99% removal efficiency maintained for 6 h. This indicated that a decrease in IPDA concentration caused a decrease in the viscosity of the mixture reduced the reaction rate for CO_2 absorption. When 5 mL of H_2O was used, it took ca. 5 h for the precipitate of carbamic acid, after which it was rapidly produced. As for the total CO_2 absorbed, IPDA aq. with a low concentration of IPDA (using 10 and 15 mL of H_2O) showed higher S_{abs} than that with a high concentration. When the amount of H_2O was 10 mL, 1.28 $mmol_{CO2}$ was captured by 1 $mmol_{IPDA}$. Thus, increasing the solvent volume from 5 to 15 mL resulted in CO_2 absorption capacity increasing beyond a CO_2:IPDA ratio of 1:1, which was attributed to the formation of bicarbonate/carbonate species as assigned in ^{13}C NMR (Supplementary Fig. S4B). The basic aqueous solution of IPDA (pH = 11.91 when 10 mL of H_2O was used) preferentially captured CO_2 as carbamic acid species. Indeed, 10 mL of NaOH aqueous solution with the same pH (11.91) showed absorption capacity of 0.1 $mmol_{CO2}$ for 400 ppm CO_2 (Supplementary Table S3).[36–38]

We also tested the dissolution limit of **CA1** in H_2O. Figure 4b shows the residual amount of solid **CA1** after dissolution of 1 mmol **CA1** into various amounts of H_2O. In the case when 1 mL of H_2O was used, the solid **CA1** remained in aqueous phase and the amount after centrifugation with acetone was 0.202 g [corresponding to 0.94 mmol as $(CH_3)_3C_6H_4(NH_2)CH_2NHCOOH$(s)], while the carbamic acid completely dissolved into 20 mL of H_2O. The residual solid **CA1** decreased with increasing H_2O and 0.017 g (ca. 0.079 mmol) of **CA1** remained when 15 mL of H_2O was used. Thus, we determined that the dissolution limit of carbamic acid of IPDA into pure H_2O was 11.20 g $L^{-1}{}_{H2O}$. The solubility of **CA1** in DMSO (2.10 g $L^{-1}{}_{DMSO}$) was measured in the same manner (Supplementary Fig. S7A); the results showed that a larger amount of **CA1** could exist in liquid phase in H_2O compared with that in DMSO. Among other diamines that formed precipitates after CO_2 absorption, **CA1** exhibited the lowest dissolution limit (Supplementary Fig. S7B–E).

To gain insights into the effect of concentration on the viscosity of IPDA aq. and its CO_2 absorption, the viscosity of various concentrations of IPDA aq. after the absorption of CO_2 was confirmed. Figure 5a summarizes the viscosity of IPDA aq. with different concentrations before and after 100% CO_2 saturation. After loading CO_2, the viscosity of 0.067 mol_{IPDA}/mL_{H2O} was only 0.95 mPa s, which was the same viscosity as pure H_2O (1.0 mPa s). However, after CO_2 loading, the viscosity of 0.5 mol_{IPDA}/mL_{H2O} IPDA changed from 1.18 to 3.26 mPa s. The viscosity reached 3.99 mPa s when using 1 mol_{IPDA}/L_{H2O} IPDA aq. As for the CO_2 removal efficiency in Fig. 4a, 1 mmol IPDA with 2 mL H_2O (C_{IPDA} = 0.5) showed the longest T_{90} value. This volcano-type trend of rate for CO_2 absorption, T_{90} value (Fig. 5a, right axis) is

strongly related to the solution viscosity and volume of sorbent solution. Based on the estimated dissolution limit of **CA1** (11.20 g/L_{H2O}), a half of formed carbamic acid was dissolved into 10 mL H_2O. As the content of H_2O decreased, the amount of **CA1** precipitate increased, resulting in the viscosity increasement. 1 mmol IPDA with 1 mL H_2O ($C_{IPDA} = 1$) showed the highest viscosity and resulted in decrease in T_{90} value, which would be due to the limitation of sorbent diffusion. The trend in T_{90} indicated the CO_2 absorption reaction efficiently occurred by a moderate increase in the viscosity of the mixture. Actually, viscosity of 0.5 mol_{IPDA}/mL_{H2O} IPDA aq. dramatically increased for the first 20 min of CO_2 absorption (Supplementary Fig. S8). In addition, IPDA aq. showed higher viscosity upon CO_2 loading compared with aqueous solutions of 1,2-cyclohexanediamine, 1,3-cyclohexanediamine, and 1,4-cyclohexanediamine that maintained liquid form during the CO_2 loading (Fig. 5b). Generally, the high viscosity of the solution reduces the rate of CO_2 absorption. In the present system, however, solid precipitation that occurs with increased viscosity promotes CO_2 absorption. As we explained in the introduction, one benefit of a solid–liquid phase change system is overcoming the limitation by equilibrium because of a typical carbamate mechanism. Secondly, the viscosity increasement by precipitate formation also led to the high absorption efficiency of IPDA. We also examined the effect of mixed diamine of IPDA and 1,2-cyclohexanediamine. The addition of 1, 2-cyclohexylamine showed a slight influence on the viscosity of IPDA aq. after sufficient absorption of CO_2 (Supplementary Fig. S9). Thus, we consider that the high viscosity came from the nature of **CA1** in aqueous media and that was hardy affected by the co-existence of the other amine.

The desorption properties of CO_2 captured by IPDA were evaluated at different temperatures. Figure 6a shows the CO_2 concentration profile at temperatures 90 °C under a flow of pure N_2 or 20% O_2–N_2 at 50 mL/min. To note that the feed gas of 400 ppm CO_2–N_2 was used for absorption, the absorbed amount of CO_2 (S_{abs}) was ca. 1.1 $mmol_{CO2}/mol_{IPDA}$ that mainly composed of **CA1** with insignificant bicarbonates. CO_2 concentration reached 1.6% at a maximum after 5 min, and thus CO_2 could be concentrated. The structure of IPDA has not changed after treatment of 20% O_2–N_2 at 90 °C and the absorption capacity retained in the second cycle (Supplementary Fig. S10). From the temperature dependency in Supplementary Fig. S11, **CA1** dispersed in H_2O could efficiently release CO_2 at 70 °C, while solid **CA1** required higher temperature as shown in the weight loss curve (Supplementary Fig. S12). The solid **CA1** vanished at 90 °C accompanied by almost 80% CO_2 desorption. We also confirmed the necessity of N_2 purging to this system (Supplementary Fig. S13). The collected CO_2 by heating the **CA1** in H_2O at 110 °C without N_2 flow was 0.45 mmol. These suggested that gas flow with low CO_2-containing gas is required for the efficient desorption of captured CO_2 due to the high CO_2 absorption ability of IPDA. In the DAC system for greenhouse plant, as introduced, CO_2-eliminated air could be obtained for sweeping gas for CO_2 desorption. To ensure the applicability of our system for plant growth, the mixing gas of N_2 and O_2 was used for desorption of CO (Fig. 6a). We also tested the recyclability of IPDA aq. and more than 50% CO_2 cycle loading (0.22 wt%) can be achieved under the flow gas of 400 ppm CO_2–N_2 for absorption and N_2 at 90 °C for desorption (Fig. 6b).

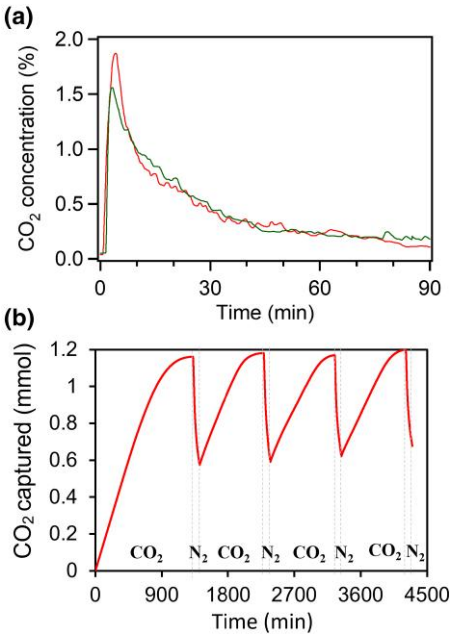

Fig. 6. a) CO_2 desorption profile from IPDA aq. at 90 °C under gas flowing after absorption of 400 ppm CO_2. For absorption: IPDA: 1.0 mmol; H_2O: 2.0 mL; F_{gas}: 400 ppm CO_2–N_2, 75 mL/min; temperature: ambient. For desorption: N_2 or 20% O_2–N_2, 50 mL/min; temperature: 90 °C. Desorption measurement under N_2 (Red line): $S_{abs} = 1.10$ mmol, $S_{dsp} = 0.89$ mmol. Desorption measurement under 20% O_2–N_2 (green line): $S_{abs} = 1.10$ mmol, $S_{dsp} = 0.89$ mmol. b) Absorption–desorption cycles over IPDA aq. (IPDA: 1.0 mmol; H_2O: 10 mL). For absorption, F_{gas}: 400 ppm CO_2–N_2, 20 mL/min; temperature: ambient. For desorption: N_2: 50 mL/min; temperature: 90 °C.

Finally, the mechanism of CO_2 absorption by IPDA in aqueous solution is discussed. IPDA aq. showed an induction period before it could reach >99% efficiency of CO_2 absorption, and the formation of **CA1** precipitate triggered this increase in efficiency (Fig. 3). At the initial stage, IPDA in aqueous solution reacted with CO_2 and formed carbamate species via a zwitterionic mechanism ($2NH_2–R–C_6H_4–NH_2(l) + CO_2(l) \rightarrow NH_2–R–C_6H_4–NH–COO^-(l) + NH_2–R–C_6H_4–NH_3^+(l)$), which is typical in aqueous MEA systems.[39,40] Indeed, theoretical calculation revealed that IPDA easily formed the zwitterion upon CO_2 addition with the low activation energy of 16.1 kJ/mol (Fig. 7, 1→2). Then, the proton of zwitterion moved to another IPDA molecule or intermolecular amino group, and a carbamate species was formed (Fig. 7, 2→3), while there was a large barrier to the formation of carbamic acid (Fig. 7, 2→4). It should be noted that the energies of 3, $TS_{3\text{-}8}$, and 8 were calculated to be almost same within the errors caused by the solution model, indicating that the proton transfer between amino groups occurs almost without barriers. In addition, the DFT calculations in this study were performed under the continuum solvation model without explicitly considering the acidity of the solution. In the actual system, the degree of dissociation of the carbamic acid will decrease with increasing the acidity by CO_2 absorption, leading to the solid precipitation. Importantly, the formation of carbamic acid from IPDA and CO_2 can proceed under H_2O solvation.[41,42] At the middle stage, the concentrations of carbamate and carbamic acid intermediates in the solution increased with time. When the concentration of carbamic acid reached the dissolution limit, carbamic acid separated out from the aqueous solution as a solid precipitate. Indeed, the viscosity increased accompanied by the formation of **CA1** (Supplementary Fig. S8).

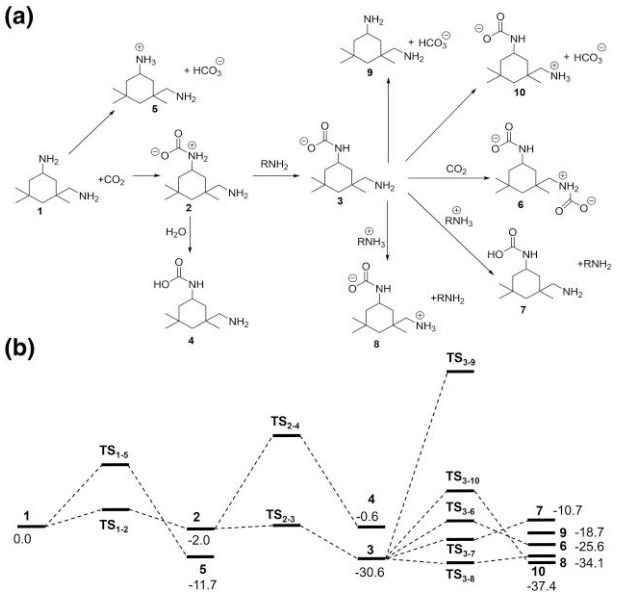

Fig. 7. a) Reaction scheme and b) energy diagram (Gibbs free energy in kJ/mol) of CO_2 absorption reaction of IPDA in aqueous solutions. The DFT calculations were carried out at the SMD/IEF-PCM/B3LYP/6-311++G(d,p) level.

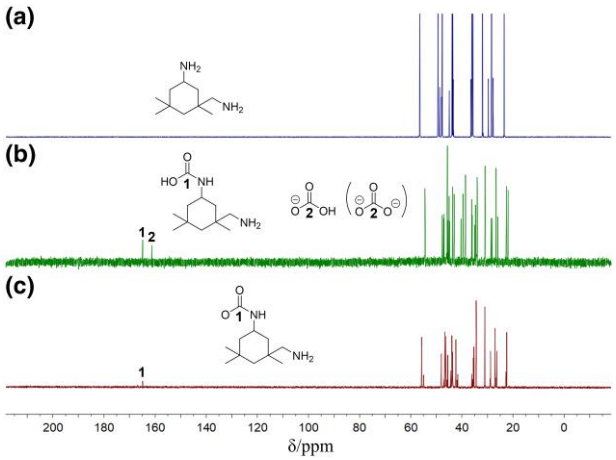

Fig. 8. ^{13}C NMR spectra measured in D_2O at 25 °C. a) Pure IPDA, b) IPDA aq. after absorption of 400 ppm CO_2 (1 mmol IPDA and 2 mL of H_2O), and c) IPDA aq. after desorption of CO_2 under N_2 at 80 °C from b).

All the routes to bicarbonate formation (Fig. 7, 1→5, 3→9, 3→10) had relatively large barriers, which may be reduced if the proton transfer in water molecules is considered. It should be noted that the energy barrier for bicarbonate formation is higher than that for carbamate formation based on the precious study for similar system.[32] However, the energy diagram shows that bicarbonate products are stable in terms of Gibbs free energies compared with the carbamate and carbamic acid. The calculation results suggest that sufficient absorption time and CO_2 loading can produce a significant amount of bicarbonate.

^{13}C NMR spectra also revealed the presence of bicarbonate/carbonate ion species after CO_2 absorption by IPDA aq. (Fig. 8b). The captured CO_2 could be released by heating under N_2 flow, and only some of the carbamate/carbamic acid species remained in the aqueous solution after heating at 80 °C (Fig. 8c). It is reported that aqueous amine system including MEA formed carbamate species initially, followed by bicarbonate/carbonate ions formation.[43,44] During the desorption, the carbamic acid of MEA remained throughout the desorption while the bicarbonate/carbonate species disappeared immediately.[45] Thus, we concluded that IPDA aq. captured CO_2 as carbamic acid initially followed by bicarbonate/carbonate formation, while the release of CO_2 in bicarbonate/carbonate ions occurred immediately during the desorption.

In this study, IPDA aq. exhibited the most efficient CO_2 removal among the various diamines in aqueous solution (Table 1 and Supplementary Fig. S2). IPDA formed **CA1** which has the lowest solubility among diamines that formed precipitate of carbamic acids (Fig. 4b and Supplementary Fig. S7), thus the large amount of **CA1** rapidly precipitated during CO_2 absorption. In addition, the viscosity of the solution increased accompanied by the formation of **CA1** (Supplementary Fig. S8). The high viscosity of the solution increased the gas-sorbent contact time. The volume of sorbent that the CO_2-containing gas passed through also changed the gas-sorbent contact time, and thus, the H_2O volume dependency of T_{90} value in Fig. 5a showed a volcano-type trend. IPDA/**CA1** aq. had higher viscosity compared to other diamines (Fig. 5b). These indicated the benefit of viscosity for efficient contact in our solid–liquid phase separation system, although the direct relationship between solution viscosity and CO_2 removal efficiency is under a debate. In particular, IPDA aq. achieved >99% CO_2 removal under 500 min^{-1} flow of 400 ppm CO_2–N_2. This high reaction rate R_{SV} of 4.46 mmol/L·min even under a high contact rate (SV = 13,761.5 h^{-1}) opens up the possibility of developing a practical, cost-efficient, and environmentally friendly DAC system using H_2O as a solvent.

Besides, we also demonstrate the CO_2 condensation using 20% O_2–N_2 gas at 90 °C from IPDA aq. after CO_2 loading. This indicated the applicability of our system to CO_2 condensation for plant growth by sweeping the CO_2-eliminated air gas. The desorption heat calculated based on the specific heat of sorbent was 530 kJ/mol_{CO2} that is lower than the reported MEA based system with a similar laboratory scale experiment (ca. 1,500 kJ/mol_{CO2}).[46,47] Actually, heating aqueous solutions costs a lot of energy compared to heating the solid itself, and thus, the further development of our DAC system for a practical use, such as the heat exchanger or heat capacitor to reduce the heat duty,[48,49] is required. This study showed that CO_2 desorption temperature from **CA1** decreased by using H_2O as a solvent. Thus, we established the proof-of-concept for DAC using solid-liquid phase separation system in an aqueous solvent. To develop the practical DAC system for greenhouse agriculture, the equipment cost and thermal management must be considered.

4. Conclusion

In summary, we demonstrated that a series of diamine aqueous solutions could capture low-concentration CO_2 (400 ppm) with high amine utilization efficiency of >1 $mmol_{CO2}/mmol_{amine}$. IPDA exhibited >99% removal efficiency of 400 ppm CO_2 for 12 h with the formation of [(aminomethyl)-3,5,5-trimethylcyclohexyl]carbamic acid precipitate and bicarbonate/carbonate species. We found that the CO_2 absorption rate depends on the viscosity of the amine solutions because the IPDA aqueous solution has higher viscosity

than other diamines. CO_2 capacity achieved 1.28 $mmol_{CO2}$/$mmol_{IPDA}$ when using low-concentration IPDA aq. due to the formation of bicarbonate/carbonate ion species. 0.5 M IPDA aq. absorbed 400 ppm CO_2 efficiently (R_{SV} = 4.46 mmol/L·min) even at a high flow rate of 500 mL/min after the solid carbamic acid was precipitated. One of the possible reasons was that the increase in slurry viscosity improves the contact of IPDA with CO_2. The absorbed CO_2 could desorb at 90 °C even under 20% O_2–N_2, which simulates CO_2-eliminated air, indicating the applicability of our system to CO_2 condensation for greenhouse agriculture. DFT calculation revealed that carbamic acid of IPDA and bicarbonate species could be formed as a result of CO_2 absorption. The ^{13}C NMR showed that the absorbed CO_2 in bicarbonate/carbonate was initially detached and some of carbamic acid of IPDA remained after heating. The above results demonstrated that IPDA aq. with a high CO_2 absorption rate and reusability in absorption and desorption cycles is a promising candidate for CO_2 absorbent for DAC system. A long stability, viscosity controlling, and system operation is still required to further research for the industrial application of this adsorbent.

Supplementary data

Supplementary material is available at *Bulletin of the Chemical Society of Japan* online. Performances of reported CO_2 sorbents and formed solid compounds' solubility and shear viscosity, ^{13}C NMR and FT-IR spectra, TG profile of solid **CA1**, and photograph of experimental set-up.

Funding

This study was financially supported by New Energy and Industrial Technology Development Organization (NEDO) (JPNP14004), JSPS KAKENHI (No. 20K22467, 21H01718, 21K18855, and 22K14543), Tokyo Metropolitan Government Advanced Research (R3-1), Tokyo Human Resources Fund for City Diplomacy, and Tokyo Metropolitan University Research Fund for Young Scientists.

Conflict of interest statement. We have no competing interests.

Data availability

The data underlying this study are available in the published article and its Supporting Information.

References

1. X. Lan, P. Tans, K. W. Thoning, Trends in Atmospheric Carbon Dioxide (Earth System Research Laboratory, Global Monitoring Division, NOAA. [accessed September 2017]. https://www.esrl.noaa.gov/gmd/ccgg/trends/global.html.
2. T. Gasse, C. Guivarch, K. Tachiiri, C. D. Jones, P. Ciais, *Nat. Commun.* **2015**, *6*, 7958. https://doi.org/10.1038/ncomms8958
3. R. M. Cuéllar-Franca, A. Azapagic, *J. CO_2 Util.* **2015**, *9*, 82. https://doi.org/10.1016/j.jcou.2014.12.001
4. M. Mikkelsen, M. Jørgensen, F. C. Krebs, *Energy Environ. Sci.* **2010**, *3*, 43. https://doi.org/10.1039/B912904A
5. C. Yuan, Y. Wang, M. F. Baena-Moreno, Z. Pan, R. Zhang, H. Zhou, Z. Zhang, *Energy Fuels* **2023**, *37*, 8883. https://doi.org/10.1021/acs.energyfuels.3c00874
6. Y. Wang, Z. Pan, W. Zhang, S. Huang, G. Yu, R. M. Soltanian, E. Lichtfouse, Z. Zhang, *Chem. Lett.* **2023**, *21*, 1951. https://doi.org/10.1007/s10311-023-01596-0
7. M. Steinberg, V.-D. Dang, *Energy Convers.* **1977**, *17*, 97. https://doi.org/10.1016/0013-7480(77)90080-8
8. C. J. Major, B. J. Sollami, K. Kammermeyer, *Ind. Eng. Chem. Process Des. Dev.* **1965**, *4*, 327. https://doi.org/10.1021/i260015a019
9. M. Erans, E. S. Sanz-Pérez, D. P. Hanak, Z. Clulow, D. M. Reiner, G. A. Mutch, *Energy Environ. Sci.* **2022**, *15*, 1360. https://doi.org/10.1039/D1EE03523A
10. X. Shi, H. Xiao, H. Azarabadi, J. Song, X. Wu, X. Chen, K. S. Lackner, *Angew. Chem. Int. Ed.* **2020**, *59*, 6984. https://doi.org/10.1002/anie.201906756
11. E. S. Sanz-Pérez, C. R. Murdock, S. A. Didas, C. W. Jones, *Chem. Rev.* **2016**, *116*, 11840. https://doi.org/10.1021/acs.chemrev.6b00173
12. J. I. L. Morison, D. W. Lawlor, *Plant. Cell Environ.* **1999**, *22*, 659. https://doi.org/10.1046/j.1365-3040.1999.00443.x
13. T. Wang, J. Huang, X. He, J. Wu, M. Fang, J. Cheng, *Energy Procedia* **2014**, *63*, 6842. https://doi.org/10.1016/j.egypro.2014.11.718
14. J. Bao, W.-H. Lu, J. Zhao, X. T. Bi, *Carbon Resour.* **2018**, *1*, 183. https://doi.org/10.1016/j.crcon.2018.08.002
15. H. A. Ahmed, Y.-X. Tong, Q.-C. Yang, *S. Afr. J. Bot.* **2020**, *130*, 75. https://doi.org/10.1016/j.sajb.2019.12.018
16. Y. Zheng, F. Li, L. Hao, A. A. Shedayi, L. Guo, C. Ma, B. Huang, M. Xu, *BMC Plant Biol.* **2018**, *18*, 18. https://doi.org/10.1186/s12870-018-1232-6
17. G. T. Rochelle, *Science* **2009**, *325*, 1652. https://doi.org/10.1126/science.1176731
18. J. Zhang, Y. Qiao, D. W. Agar, *Energy Procedia* **2012**, *23*, 92. https://doi.org/10.1016/j.egypro.2012.06.072
19. J. M. Hanusch, I. P. Kerschgens, F. Huber, M. Neuburger, K. Gademann, *Chem. Commun.* **2019**, *55*, 949. https://doi.org/10.1039/C8CC08574A
20. F. Barzagli, C. Giorgi, F. Mani, M. Peruzzini, *ACS Sustain. Chem. Eng.* **2020**, *8*, 14013. https://doi.org/10.1021/acssuschemeng.0c03800
21. F. Barzagli, M. Peruzzini, R. Zhang, *Carbon Capt. Sci. Technol.* **2022**, *3*, 100049. https://doi.org/10.1016/j.ccst.2022.100049
22. J. M. Kolle, M. Fayaz, A. Sayari, *Chem. Rev.* **2021**, *121*, 7280. https://doi.org/10.1021/acs.chemrev.0c00762
23. F. Inagaki, C. Matsumoto, T. Iwata, C. Mukai, *J. Am. Chem. Soc.* **2017**, *139*, 4639. https://doi.org/10.1021/jacs.7b01049
24. S. W. Lee, S. W. Lim, S. H. Park, K. Ha, K. S. Kim, S. M. Oh, J. Y. Lee, G. Seo, *Korean J. Chem. Eng.* **2013**, *30*, 2241. https://doi.org/10.1007/s11814-013-0171-z
25. M. K. Leszczyński, D. Kornacki, M. Terlecki, I. Justyniak, G. I. Miletić, I. Halasz, P. Bernatowicz, V. Szejko, J. Lewiński, *ACS Sustain. Chem. Eng.* **2022**, *10*, 4374. https://doi.org/10.1021/acssuschemeng.1c08402
26. A. Kasturi, J. Gabitto, C. Tsouris, R. Custelcean, *Sep. Purif. Technol.* **2021**, *271*, 118839. https://doi.org/10.1016/j.seppur.2021.118839
27. H. Cai, X. Zhang, L. Lei, C. Xiao, *ACS Omega* **2020**, *5*, 20428. https://doi.org/10.1021/acsomega.0c02460
28. F. M. Brethomé, N. J. Williams, C. A. Seipp, M. K. Kidder, R. Custelcean, *Nat. Energy* **2018**, *3*, 553. https://doi.org/10.1038/s41560-018-0150-z
29. K. A. Garrabrant, N. J. Williams, E. Holguin, F. M. Brethomé, C. Tsouris, R. Custelcean, *Ind. Eng. Chem. Res.* **2019**, *58*, 10510. https://doi.org/10.1021/acs.iecr.9b00954
30. S. Kikkawa, K. Amamoto, Y. Fujiki, J. Hirayama, G. Kato, H. Miura, T. Shishido, S. Yamazoe, *ACS Environ. Au* **2022**, *2*, 354. https://doi.org/10.1021/acsenvironau.1c00065
31. A. V. Marenich, C. J. Cramer, D. G. Truhlar, *J. Phys. Chem. B* **2009**, *113*, 6378. https://doi.org/10.1021/jp810292n
32. H. Yamada, Y. Matsuzaki, T. Higashii, S. Kazama, *J. Phys. Chem. A* **2011**, *115*, 3079. https://doi.org/10.1021/jp109851k
33. H. Yamada, *J. Phys. Chem. B* **2016**, *120*, 10563. https://doi.org/10.1021/acs.jpcb.6b07860

34. M. J. Frisch, G. W. Trucks, H. B. Schlegel, G. E. Scuseria, M. A. Robb, J. R. Cheeseman, G. Scalmani, V. Barone, G. A. Petersson, H. Nakatsuji, X. Li, M. Caricato, A. V. Marenich, J. Bloino, B. G. Janesko, R. Gomperts, B. Mennucci, H. P. Hratchian, J. V. Ortiz, A. F. Izmaylov, J. L. Sonnenberg, D. Williams-Young, F. Ding, F. Lipparini, F. Egidi, J. Goings, B. Peng, A. Petrone, T. Henderson, D. Ranasinghe, V. G. Zakrzewski, J. Gao, N. Rega, G. Zheng, W. Liang, M. Hada, M. Ehara, K. Toyota, R. Fukuda, J. Hasegawa, M. Ishida, T. Nakajima, Y. Honda, O. Kitao, H. Nakai, T. Vreven, K. Throssell, J. A. Montgomery Jr, J. E. Peralta, F. Ogliaro, M. J. Bearpark, J. J. Heyd, E. N. Brothers, K. N. Kudin, V. N. Staroverov, T. A. Keith, R. Kobayashi, J. Normand, K. Raghavachari, A. P. Rendell, J. C. Burant, S. S. Iyengar, J. Tomasi, M. Cossi, J. M. Millam, M. Klene, C. Adamo, R. Cammi, J. W. Ochterski, R. L. Martin, K. Morokuma, O. Farkas, J. B. Foresman, D. J. Fox, GaussView 5.0. Wallingford, E.U.A., Gaussian, Inc., Wallingford CT, 2016.
35. T. Wang, J. Liu, K. S. Lackner, X. Shi, M. Fang, Z. Luo, *Greenh Gases* **2015**, *6*, 138. https://doi.org/10.1002/ghg.1535
36. J. K. Stolaroff, D. W. Keith, G. V. Lowry, *Environ. Sci. Technol.* **2008**, *42*, 2728. https://doi.org/10.1021/es702607w
37. K. S. Lackner, *Eur. Phys. J. Special Top.* **2009**, *176*, 93. https://doi.org/10.1140/epjst/e2009-01150-3
38. M. Saeidi, A. Ghaemi, K. Tahvildari, P. Derakhshi, *J. Chin. Chem. Soc.* **2018**, *65*, 1465. https://doi.org/10.1002/jccs.201800012
39. H.-B. Xie, Y. Zhou, Y. Zhang, J. K. Johnson, *J. Phys. Chem. A* **2010**, *114*, 11844. https://doi.org/10.1021/jp107516k
40. N. McCann, D. Phan, X. Wang, W. Conway, R. Burns, M. Attalla, G. Puxty, M. Maeder, *J. Phys. Chem. A* **2009**, *113*, 5022. https://doi.org/10.1021/jp810564z
41. Y. Zheng, S. Zhang, Y. Liu, C. Wang, B. Lv, G. Jing, Z. Zhou, *Sep. Purif. Technol.* **2023**, *313*, 123486. https://doi.org/10.1016/j.seppur.2023.123486
42. D. Wei, Q. Luo, T. Ouyang, Q. Liu, Y. Huang, B. Jin, H. Gao, X. Luo, Z. Liang, *AIChE J.* **2023**, *69*, e17960. https://doi.org/10.1002/aic.17960
43. F. Barzagli, C. Giorgi, F. Mani, M. Peruzzini, *Ind. Eng. Chem. Res.* **2019**, *58*, 4364. https://doi.org/10.1021/acs.iecr.9b00552
44. R. Zhang, X. Luo, Q. Yang, H. Yu, G. Puxty, Z. Liang, *Int. J. Greenh. Gas Con.* **2018**, *71*, 1. https://doi.org/10.1016/j.ijggc.2018.02.001
45. B. Lv, B. Guo, Z. Zhou, G. Jing, *Environ. Sci. Technol.* **2015**, *49*, 10728. https://doi.org/10.1021/acs.est.5b02356
46. X. Zhang, H. Liu, Z. Liang, R. Idem, P. Tontiwachwuthikul, M. J. Al-Marri, A. Benamor, *Appl. Energy* **2018**, *229*, 562. https://doi.org/10.1016/j.apenergy.2018.07.035
47. X. Zhang, X. Zhang, H. Liu, W. Li, M. Xiao, H. Gao, Z. Liang, *Appl. Energy* **2017**, *202*, 673. https://doi.org/10.1016/j.apenergy.2017.05.135
48. P. Niegodajew, D. Asendrych, S. Drobniak, *J. Power Technol* **2013**, *93*, 354.
49. Y. S. Yu, H. F. Lu, T. T. Zhang, Z. X. Zhang, G. X. Wang, V. Rudolph, *Ind. Eng. Chem. Res.* **2013**, *52*, 12622. https://doi.org/10.1021/ie400353f